Tectonics

RESEARCH ARTICLE
10.1029/2019TC006014

Key Points:
- The complex and diffuse fault segmentation of fault system derives from intense preexisting crustal heterogeneity
- Large-magnitude earthquakes along the system are related to broad high Vp/Vs overpressurized volumes at the base of the seismogenic layer
- Monitoring of this target will help decipher the interaction between deep fluids and seismicity before and during major seismic sequences

Supporting Information:
- Supporting Information S1

Correspondence to:
C. Chiarabba,
claudio.chiarabba@ingv.it

Citation:
Chiarabba, C., Buttinelli, M., Cattaneo, M., & De Gori, P. (2020). Large earthquakes driven by fluid overpressure: The Apennines normal faulting system case. *Tectonics*, *39*, e2019TC006014. https://doi.org/10.1029/2019TC006014

Received 2 DEC 2019
Accepted 2 MAR 2020
Accepted article online 5 MAR 2020

Large Earthquakes Driven by Fluid Overpressure: The Apennines Normal Faulting System Case

C. Chiarabba[1], M. Buttinelli[1], M. Cattaneo[1], and P. De Gori[1]

[1]Istituto Nazionale di Geofisica e Vulcanologia, Rome, Italy

Abstract Fluid overpressure is a primary mechanism behind fault interaction and earthquakes triggering. The Apennines section within the young Alpine mobile belt is a key locus to investigate the interplay between fluids and faults. Here, seismicity develops along the extending mountain belt and the key role of fluids has been invoked in past large earthquake sequences. In this study, we use seismological data to get improved images of the Apennines normal faulting system, trying to catch evidences for the involvement of fluids in the preparatory phase of large earthquakes. We observe that extension preferentially reutilizes inherited fragments of faults which were assembled during the Mio-Pliocene contraction, with steep segments that floor on a regional-scale gently east dipping plane. We find evidences for wide volumes of overpressured fluids at the base of the seismogenic layer, which are connected to the activation of the recent large earthquakes. The recognition of fluids compartments with overpressuring and diffusion molding seismicity is a key to understand faulting processes and possibly develop forecasts scenarios.

Plain Language Summary We present the first full image of the deep structure of the paradigmatic normal faulting system of the Apennines, obtained by an impressive set of seismological data collected during seismic sequences originated in the past two decades. The synoptic view permits to explore the interaction between earthquakes and fluids within the crust. Such interaction is every day more important because fluid pressure changes in the subsurface (even created by human activities) might trigger large earthquakes even at a distance. The novelty of our results is the imaging of deep fluids at the base of the extensional fault system in the Apennines related to the development of all the large earthquakes that occurred over the two decades. This finding breaks through a persistent problem in earthquake preparation processes and has clear implications for tectonics of extensional systems, inversion tectonics, physics of earthquakes, and aftershock forecasting.

1. Introduction

The way in which faults interact and suddenly fail in complex and prolonged seismic sequences is a challenging issue in seismology. Increasing pore pressure is seen as a valid triggering mechanism for earthquakes (Raleigh et al., 1976; Stein, 1999), and fault lubrication is well documented in laboratory experiments (De Paola et al., 2011; Di Toro et al., 2011; Hainzl et al., 2006; Reches & Lockner, 2010; Sleep & Blanpied, 1992). Fluid diffusion can assist the onset and development of aftershocks and complex seismic sequences (Miller et al., 2004; Nur & Booker, 1972; Zhao et al., 2015) and is invoked at various scales to explain seismicity migration (Parotidis et al., 2003; Shapiro et al., 2003), changes in seismicity rate (Hainzl & Ogata, 2005; Llenos & Michael, 2016), and fault reactivation during fluid injection (Guglielmi et al., 2015; Improta et al., 2017; Peterie et al., 2018; Zoback & Harjes, 1997). High pore pressure in proximity of mainshock hypocenters is inferred from indirect imaging of the fault (Zhao et al., 1996; Chiarabba & De Gori, 2009), while in induced seismicity cases correlation with industrial data and modeling provide validation of fluid-governed processes (Keranen et al., 2014; Yeck et al., 2016; Yu et al., 2019).

While fluids in the earthquake generation process are well documented (Shapiro, 2015), capturing their involvement in the incipient phase of a large earthquake remains a challenging issue. In this study, we use the cascading earthquakes sequence originating along the Apennines normal faulting system (Figure 1) to investigate the role of fluids in the earthquake generation. Since the extension rate across the Apennines is low, 2–3 mm/yr (D'Agostino et al., 2014), resulting in about 0.02 bar/yr of stress rate, the crude occurrence of numerous $M > 5$ earthquakes over a limited time window (Figure 1) might have been favored by fluid-assisted triggering processes. At a regional scale, the deep leakage of fluids from the mantle has been

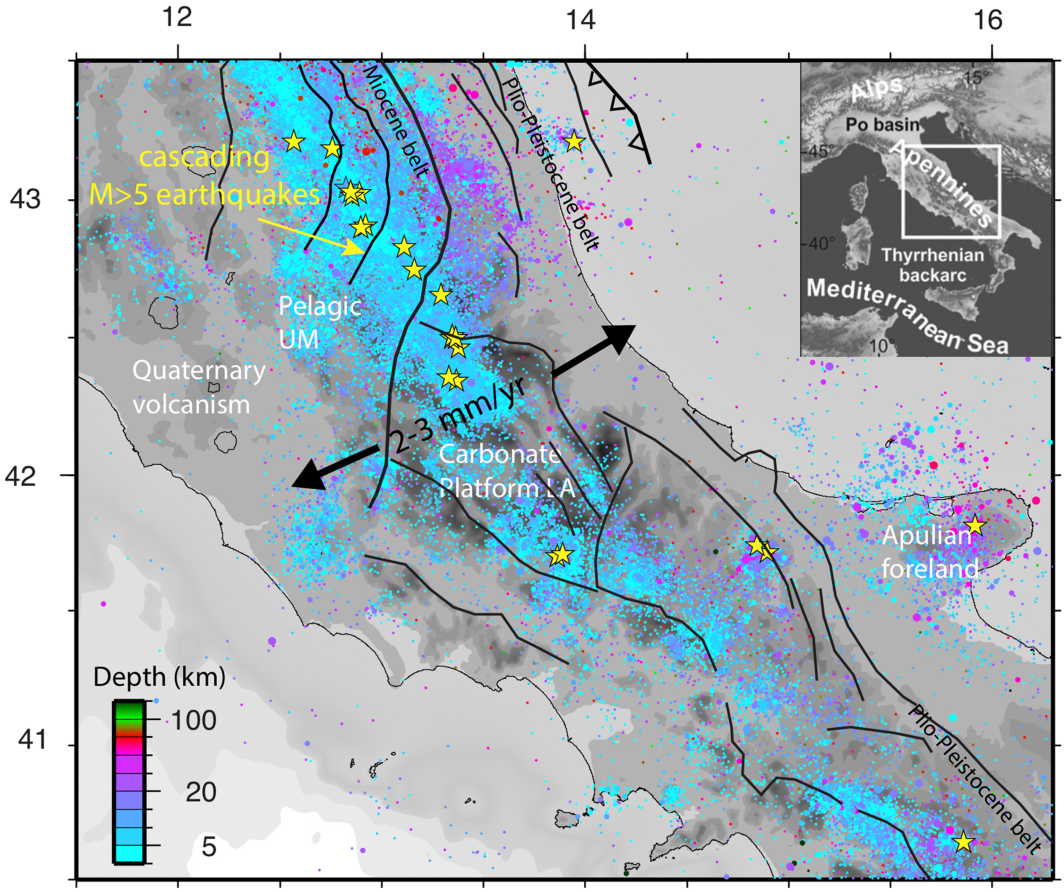

Figure 1. Seismotectonic sketch of the study area: The spine of normal faulting system along the Apennines belt. Yellow stars are earthquakes with $M_l > 5.0$ that occurred since 1984. Main compressional tectonic lineaments modified from Bigi et al. (2011) and Barchi et al. (2012). Present-day belt-normal extension of about 2–3 mm/yr from D'Agostino et al. (2014).

related to seismicity (Chiodini et al., 2004), as part of a broad process of lithospheric delamination (Chiarabba & Chiodini, 2013). At a local space-time scale, change in fluid pressure has been proposed to explain change in background seismicity rate (Lombardi et al., 2010) and fault failure of mainshock and large aftershocks (Lucente et al., 2010; Miller et al., 2004; Chiarabba & De Gori, 2009; Savage, 2010; Baccheschi et al., 2019).

The concomitance of such processes with the availability of high-quality data accumulated through the years by permanent and temporary seismic surveys candidate the Apennines normal fault system as the ideal natural laboratory to explore the relation between earthquakes and fluids. To get enhanced images of the fault system structure, we integrate all data acquired during the numerous dense seismic monitoring experiments (Figure 2). While the data sets were previously used separately to focus on individual segments (e.g., Carannante et al., 2013; Chiarabba & Amato, 2003; Di Stefano et al., 2011), their integration allows us to improve the tomographic imaging over the entire fault system. Long distance raypaths and abutting data increase and extend the model resolution to the deep seismogenic portion and how it roots in the middle-lower crust, regions that are usually undersampled and poorly known. Integration of data also gives unprecedented details of the overall belt architecture, recognizing how the present-day tectonics interferes with crustal heterogeneity and structures mostly developed during the Mio-Pliocene contractional orogeny buildup and even in previous tectonic stages.

2. Data and Model Inversions

The recordings of seismicity during major sequences and experiments in the past two decades by dense seismic networks makes it possible to create a fully comprehensive set of *P* and *S* wave arrivals that illuminate

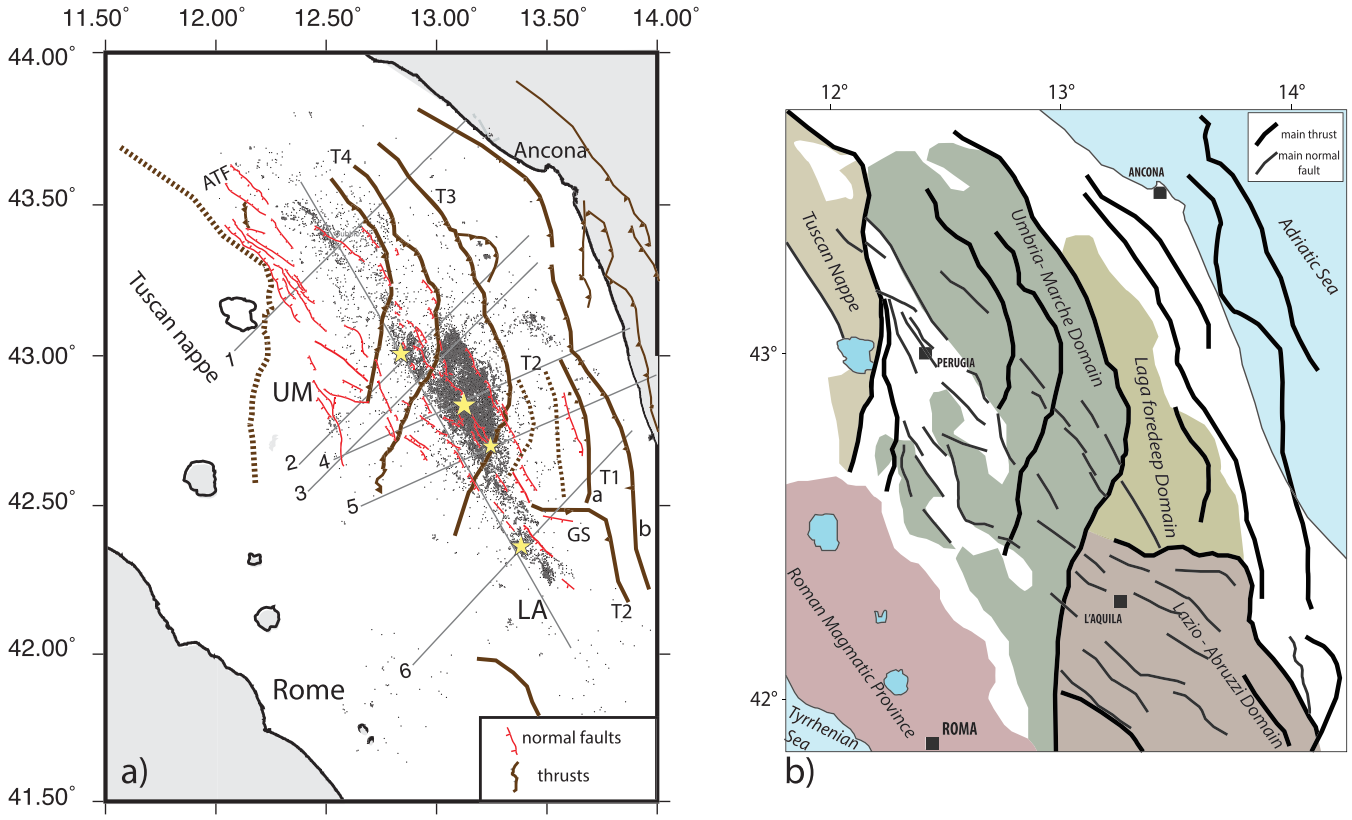

Figure 2. (a) Seismicity used in this present study, coming from a collection of temporary and permanent networks data. The main compressional lineaments are shown coded (T5–T1) according to Bigi et al. (2011). Red lines are normal faults. Yellow stars are the mainshocks of the 1997 (M_w5.9), 2009 (M_w6.1), and 2016 (M_w6.1, 6.5) sequences. Traces of vertical sections in Figure 6 are shown. (b) Simplified geologic map showing the main structural domains and structures.

the entire section of the central Apennines faulting system (Figure 3). The total data set is the richer ever assembled and used and enclose data from: Colfiorito 1997 (Chiarabba & Amato, 2003), L'Aquila 2009 (Di Stefano et al., 2011) and Norcia-Amatrice 2016 (Chiarabba et al., 2018) seismic sequences, and the Alto Tiberina Fault experiment (ATF see Valoroso et al., 2017; Carannante et al., 2013) and Firb project 2003–2005 (Chiarabba et al., 2010) experiments. All previous studies illuminate portions of the system that is well recovered in its entirety for the first time in this study.

The tomographic model is computed using the Simulps14 code (Haslinger, 1998). *P* and *S-P* arrival times are simultaneously inverted for hypocentral, Vp and Vp/Vs parameters in a linearized iterative damped least squares inversion. The model is parameterized by a 3-D grid of nodes with velocity continuously defined through the volume using a linear interpolation between adjacent nodes. Seismic rays are traced using a pseudobending method, while the shooting method is used for longer raypaths.

We compute two distinct inversions: one with the entire data set and one with data acquired before the last 2016 seismic sequence (Model A and Model B, respectively). The scope of this latter inversion is to verify if peculiar anomalies in the hypocentral region of the 2016 mainshocks were identifiable before the events.

2.1. Model A: Entire Period 1997–2017

The inversion has been done using 27,653 earthquakes recorded at 551 stations (Figure 3). To compute velocity parameters on a 3-D grid with nodes every 6 × 6 × 3 km, 697,856 *P* and 593,795 *S-P* arrivals are used. The average number of *P* and *S* wave arrivals is different for each individual data set, and the total number of seismic stations is achieved summing up the data sets, while the maximum number of stations for an event is anyway less than 90. A final root-mean-square error (rms) of 0.13 s and a variance improvement equal to 52% have been achieved after six iterations.

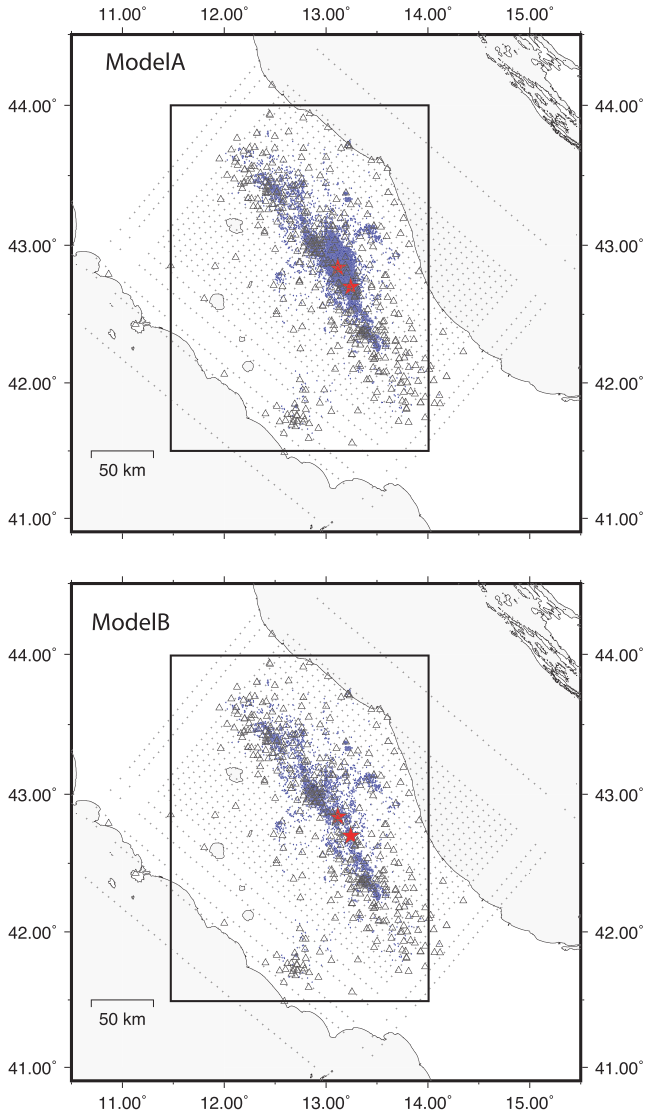

Figure 3. Setup of the Model A and Model B inversions. Used earthquakes (blue dots), seismic stations (triangles), and grid nodes (crosses) are shown. The rectangle shows the part of the model presented in Figures 4, 5, and 7. The red stars are the two mainshocks that occurred in 2016.

2.2. Model B: 1997–2015

This inversion has been done using a subset of data that span the period before the Amatrice 2016 earthquakes (Figure 3). From 6,856 earthquakes recorded at 520 stations, 188,419 *P* and 133,154 *S-P* arrivals have been used. A final rms of 0.13 s and a variance improvement equal to 58% have been achieved after six iterations.

2.3. Model Resolution

Model resolution is estimated quantitatively from the state-of-the-art analysis of the resolution matrix and spread function (SF) that contains information on the volumetric estimate of parameters. A node to be well resolved should have a compact averaging vector with elements close to 1 on the diagonal and to 0 elsewhere. The SF makes it possible to quantify the sharpness of averaging vectors, with smaller values indicating good resolution of model parameters. The smaller the SF value, the better the resolution for the model parameter. The complete maps of SF are reported in the supporting information. We report in Figure 4 the contouring, at each node, of the volume where the resolution is 70% of the diagonal element, for the Vp and Vp/Vs models at 6 km depth for the two inversions. This condition holds for well-resolved nodes, for which the estimation is picked on the diagonal element of the resolution matrix. The resolution at this key depth where the lateral heterogeneity along the Apennines is dominant, as well as in a broad portion of the model (see supporting information Figures S1–S6), is very high.

3. Results and Model Interpretation

We present and discuss the main features of the high-resolution images resolved over the 200 km long section of the normal fault system. Figure 5 shows Vp and Vp/Vs maps that reveal significant difference in velocity between the western and eastern side and the northern and southern sectors. While the former reflects the difference in thrust unit imbrication and the widespread foredeep infillings, the latter is relative to different setting between the Umbria and the Abruzzi structural domains. High Vp and Vp/Vs at 3 to 6 km depth follows the elongation of sedimentary thrust units, while a drastic change at depth below 6 km between the two domains is observed, with very high velocity prevailing in the southern area (HV in Figure 5).

The interpretation of velocity anomalies takes advantage of the available seismic and geologic information and measurements of rock velocities in laboratory (Trippetta et al., 2010). *P* and *S* wave velocities are sensitive to several factors including porosity, temperature, and pore and effective pressure, but in the upper crust lithology prevails as confirmed by previous studies (Chiarabba & Amato, 2003). The lithology in the Apennines consists of flysch foredeep units overlying a carbonate multilayer, varying from platform (LA) to deep basinal (UM). The total thickness of the sedimentary pile ranges from 2 to 6 km and lies upon a permo-Triassic basement of ambiguous nature, as it does not crop out (Bally et al., 1986). Carbonate rocks of the Apennines exhibit relatively high Vp and high Vp/Vs at elevated confining pressure (5.9–6.1 km/s and 1.9, respectively; see Trippetta et al., 2017), with values generally higher than in sandstones. Lab measurements for dolostones report Vp values as high as 7.0 km/s, but mesoscale fracturing probably limits the in situ values to 6.3 km/s, value similarly defined by tomographic estimates (Trippetta et al., 2010).

Pore geometry and fluid compressibility have strong influence on changes in Vp/Vs with increasing fluid content (Takei, 2002). Relevant for our study and of primary importance to get insight on fluids in the crust, the Vp/Vs ratio is a signature distinct of high pore pressure volumes (Dvorkin et al., 1999). The effect of pore

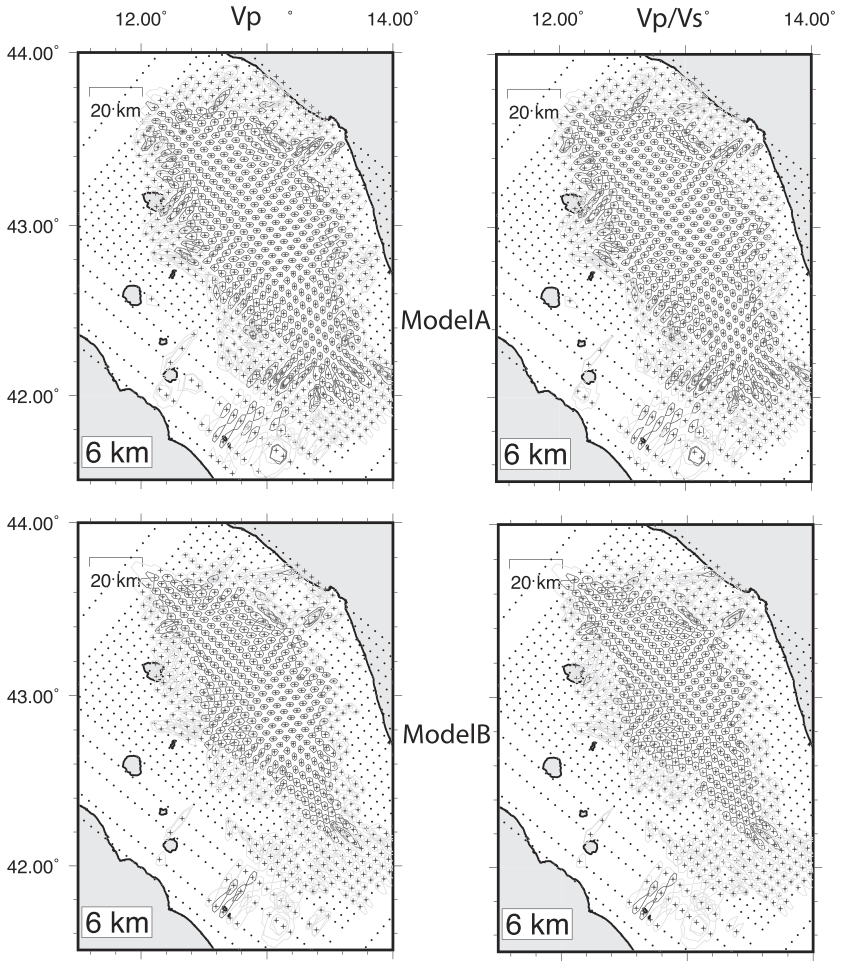

Figure 4. Model resolution for layers at 6 km depth for Vp, Vp/Vs, and for Model A and Model B (similar maps for all the other layers are reported in the supporting information). The 70% smearing contouring for inverted nodes with a spread function (SF) lower than or equal to 3.0 is shown. The nodes with SF > 1.50 and with SF < 1.50 have black and gray crosses and contours, respectively.

pressure is to counteract that of confining pressure by sustaining open pore space and cracks (Nur & Booker, 1972), lowering the velocities as a function of pore space aspect ratio (Takei, 2002). High Vp/Vs are generally interpreted as evidence for the presence of overpressured fluids (Baccheschi et al., 2019, and references therein).

We associate high Vp and high Vp/Vs to fluid-filled carbonate multilayer forming the backbone of the thrust and fold belt, normally hosting large shallow acquires (Improta et al., 2014). At greater depths, low Vp and low Vp/Vs zones in the northern portion of the area (the UM domain, Figure 1) can be related to the Permian silicic basement (e.g., Barchi et al., 2012, and reference therein), while exceptionally high Vp and relatively low Vp/Vs found in the southern part can be associated with a rigid basement whose nature is still ambiguous and largely debated so far (Chiarabba et al., 2010; Mancinelli et al., 2019).

The high Vp anomalies observed in the study area generally follow the trend of principal thrusts at surface (Figure 5), with a southwestward rotation of the more internal systems, while the external ones regain the direction orthogonal to the orogeny contraction. A main lateral heterogeneity is evident observing the velocity anomalies at depth below 6 km, which clearly divide two distinct sectors roughly from north to south. Such a large crustal discontinuity has been already invoked to describe a paleogeographic architecture before the Apennine buildup phase that evolved during Jurassic-Cretaceous times as distinct realms of the Tethys margin: the large Bahamian-type carbonate platform (LA) to the east, and the basin (UM) to the west, separated by the Ancona-Anzio lithospheric discontinuity (AAL, Tavarnelli et al., 2004).

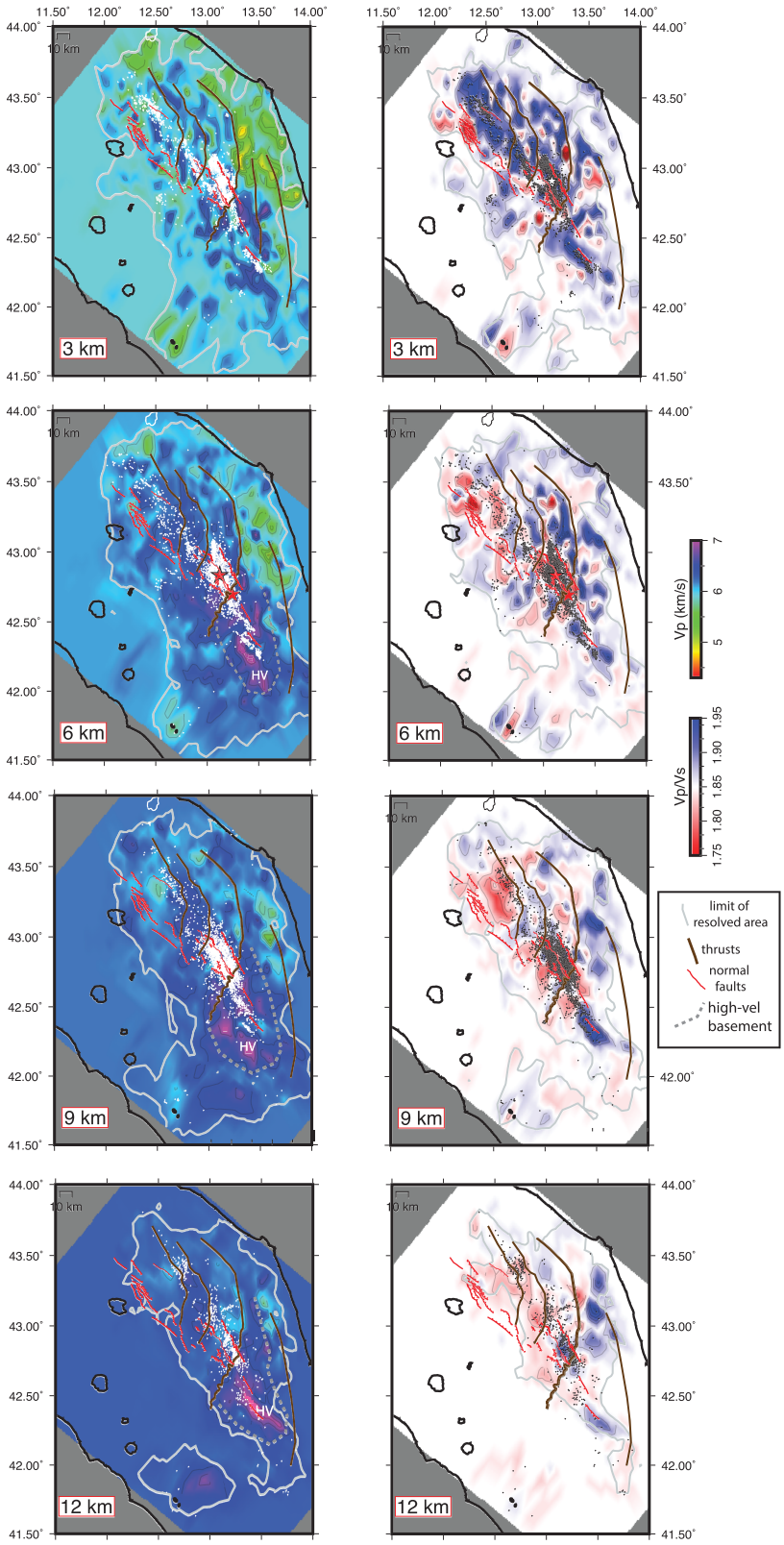

Figure 5. Velocity model of the area (Vp and Vp/Vs) with relocated seismicity occurring at ±1.5 km from each layer. Gray lines are the SF = 3.0, indicative of good resolution (see Figure 4). The red stars are the two mainshocks that occurred in 2016. Red and brown lines shown in the first layer are the normal and compressional faults (see Figure 2). In the other layers only the T2 fault is represented coinciding with the regional transition between the UM and LA domains of central Apennines. Dashed gray line indicates the limit of the rigid high-velocity basement (HV).

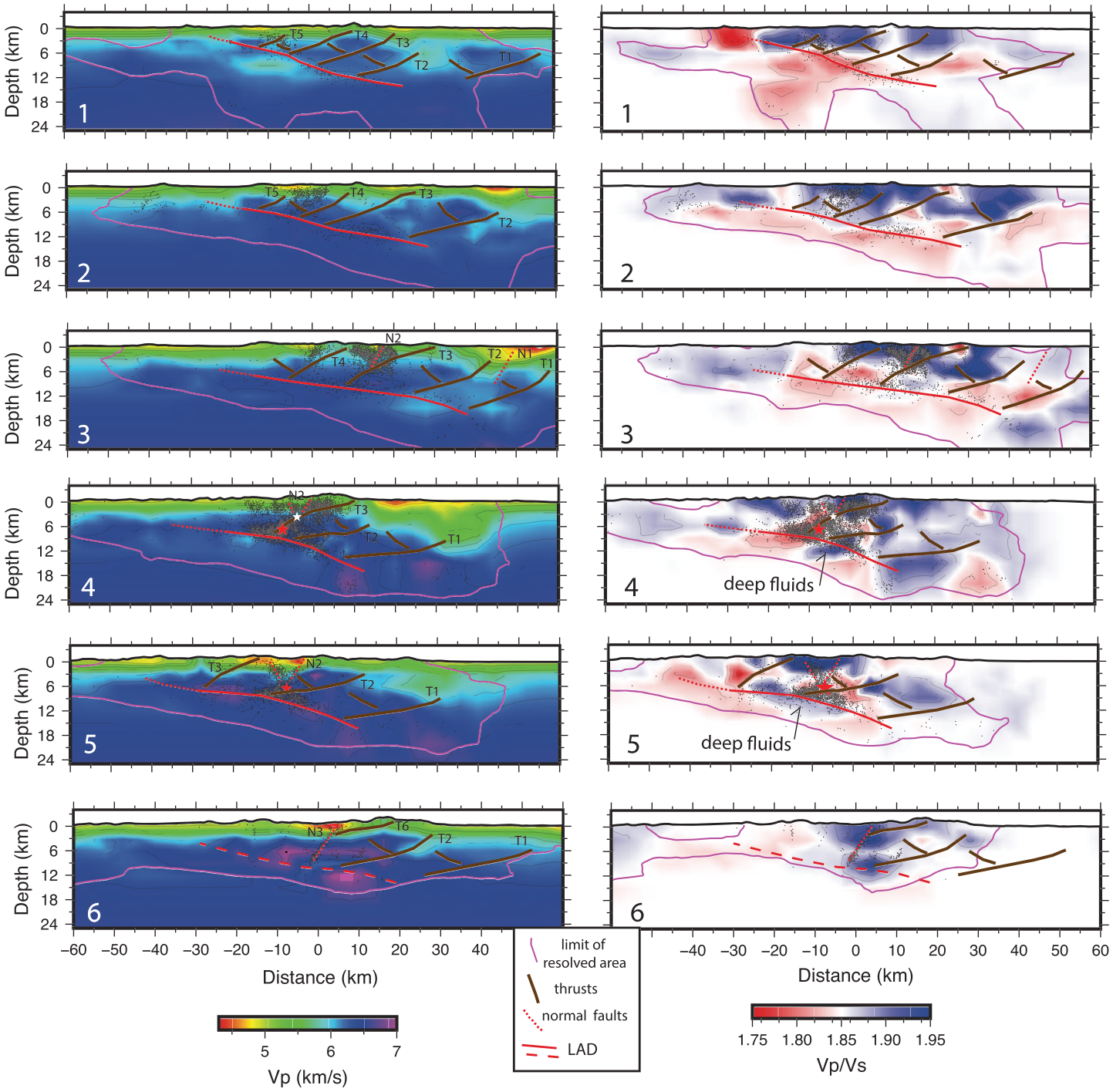

Figure 6. Vertical sections of Vp and Vp/Vs models across the main sectors of the normal faulting system (traces in Figure 2). Relocated seismicity is plotted along with the geometry of the main compressional faults, consistent with geologic sections (Barchi et al., 2012; Bigi et al., 2011). LAD = low angle detachment, like the ATF (Mirabella et al., 2011). Purple lines are the limit of the resolved region (SF = 3.0). The red stars are the two mainshocks that occurred in 2016.

Figure 6 shows Vp and Vp/Vs sections across the belt, outlining the preserved geometry of the thrust units, likely assembled in progressive and in-sequence east verging stacks. In the more external eastern area, low Vp values are associated with thick silicoclastic successions and a pronounced flexure of the carbonate substratum, which are associated with a thrust stack and recent Plio-Quaternary foredeep domains (Bally et al., 1986; Bigi et al., 2011; Lavecchia et al., 1994).

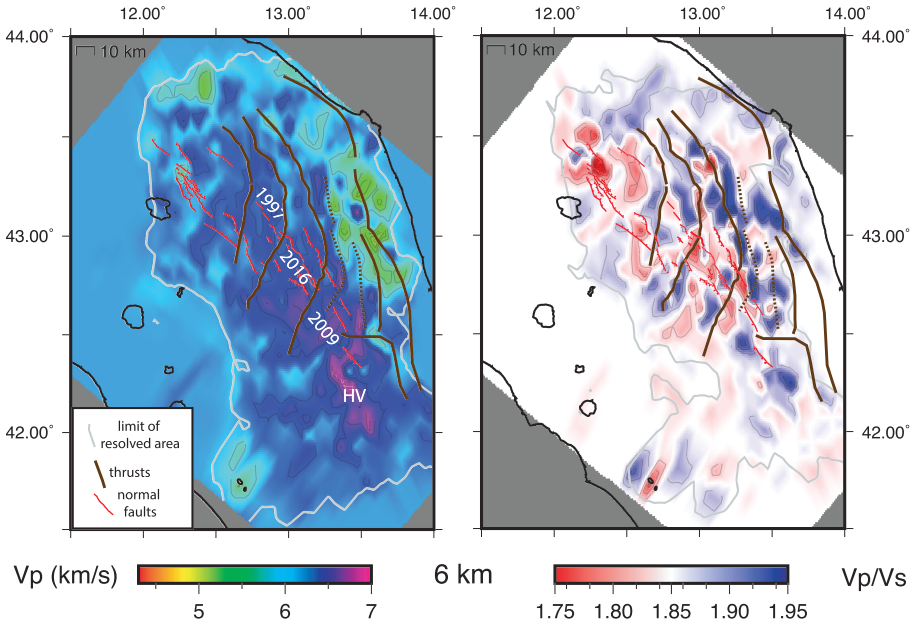

Figure 7. Velocity model at 6 km depth, with compressional and extensional structures (brown and red lines). Note that high Vp and Vp/Vs anomalies are delimited by the main thrust faults, indicating the fluids compartments in the upper crust follow the compressional structures. Extensional segments and seismic sequences are influenced and partially interrupted by the compressional system.

4. Fault System Structure and Architecture

The Apennines are a perfect example of extension overprinting and progressively spreading across a contractional belt, shortly after its formation. The central part of the belt has been built since late Miocene throughout the progressive east verging stacking of large-scale thrust sheets (e.g., Vezzani et al., 2010; Bigi et al., 2011, Figure 2), which involved in turn the paleogeographic domains of the Tuscan basin, the Lazio-Abruzzi carbonate platform (LA) and the Umbria-Marche basin (UM). Thrust sheet imbrication was accompanied by a flexure of the continental lithosphere in the external foreland and frontal shortening. Deformation rates through time are consistent with the 2–3 mm/yr present tectonic rates (D'Agostino et al., 2014). Thrusts developed following the flection of the whole arc from the Po plain to the Adriatic off-shore southward, NNW trending in the innermost areas, turning into NW-SE and more pronounced N-S directions in the external areas of the central Apennines, respectively (see also Figure 2).

Velocity tomograms show that the upper crustal structure is still dominated by the large-scale architecture of the compressional system. The pattern of velocity contrasts defines kilometer-scale systems of east verging thrusts (Figures 6), with a geometry consistent with that interpreted from seismic profiles (Barchi et al., 2012; Bigi et al., 2011; Scisciani et al., 2014). From west to east, we recognize distinct thrust sheets mostly rooted on a gently east dipping plane. Thrusts seem to have developed in a generally in-sequence propagation, characterized by younger thrusting episodes progressively propagating to the more external domains.

We generally identify four principal and broad scale episodes, which we associated to stages of deformation already recognized in literature (phases numbered according to Bigi et al., 2011):

- T5–T4 phase: formation of NNW trending thrusts in the UM domain and formation of a large foredeep (e.g., Marnoso-Arenacea);
- T3 phase: development of the large-scale Sibillini thrust accompanied by foredeep sedimentation (e.g., Laga basin), with compression that partially reworked preexisting discontinuities among the UM and LA structural domains;
- T2 phase: development of the Gran Sasso thrust system in the LA domain, propagating northward and interacting with the T3 thrusts, as clearly highlighted by tomograms.

- T1 phase: eastward progress of compression, with the development of the large Acquasanta, Montagna dei fiori and Teramo thrusts, characterized by large horizontal transport, supporting the high topography associated to the Montagna dei Fiori, Gorzano and the Gran Sasso ranges.

The progressive involvement of the sedimentary successions in the wedge was controlled by rheology of the crust. The change of velocities north and south of the AAL documents a first-order lateral heterogeneity of the midcrust along the Apennines (Figures 5–7), which we interpret as the main legacy of the Tethys realm. In the UM pelagic domain (north of AAL), velocities are consistent with the relatively thin carbonate multilayer bottomed by high-velocity Triassic evaporites and low Vp, low Vp/Vs basement (Figure 3). Conversely in the LA domain south of AAL, the carbonate multilayer is thicker and exceptionally high Vp and high Vp/Vs bodies extend in the midcrust, suggesting the presence of strong basement.

Although the role and involvement of the basement in the evolution of the thrust system is widely debated (Bigi & Costa Pisani, 2005; Butler et al., 2004; Calamita et al., 2003; Mazzoli et al., 2002; Scisciani et al., 2014; Tavarnelli et al., 2004), our images support the idea that the orogeny evolution has been controlled by a first-order midcrustal heterogeneity, presumably forming a structural high limited by high-angle faults. This body acted as a main impediment during the thrust propagation, hampering the development of deeper thrust decollements, favoring regional rotations of thrust fronts during their propagation and the development of steep ramps, also through the reworking of previous large-scale normal faults, or even the overcoming of structural highs in foreland positions. Once the compression progressed eastward and outward of the high-velocity basement (T1 phase), thrusts developed with a more efficient horizontal propagation.

This lateral heterogeneity permeating the crust exerts a key role also in the present-day belt-perpendicular extension. The main impact is on the vertical and lateral continuity and length of normal faults, which vary north and south of the AAL. The deepening of the decollement south of the AAL implies also a change in the depth of the fault's cutoff, while the obliquity of thrust ramps influences the segmentation of normal faults and the compartments of fluids within the compressional structures (Figure 5).

5. Discussion

The capability of fluids to trigger earthquakes has been known for decades (Nur & Booker, 1972; Healy et al., 1968; Raleigh et al., 1976; Sibson, 2014), but a deep understanding of such process and a collection of robust observables are still limited for large events or prolonged seismic sequences. At local scale, pressure diffusion triggering seismicity at a distance of more than 90 km from where the original pressure unbalance has been invoked (Peterie et al., 2017; Keranen et al., 2014). At regional scale, it is a main issue to address if and how a similar process could trigger large earthquakes. The involvement of fluids and pressure diffusion within the crust can produce observable and measurable parameters, monitoring of which could be an aid to forecasting seismicity occurrence. We use the central Apennines natural laboratory to investigate this relation, taking advantage of the vast data set accumulated during the peculiar decade-lasting failure of the entire faulting system.

The bricolage of faults in the study sector of the Central Apennines, partially misoriented with respect to the current extensional stress field, creates a structural complexity that is today conditioning the occurrence of large earthquakes (Chiaraluce et al., 2017). This extreme segmentation favors the accommodation of extension with cascading sequences of large shocks (the numerous $M > 5$ earthquakes that occurred in the last 20 yr) under the efficient interaction between neighboring faults. Although some authors investigated the contribution of static or dynamic stress transfer to propagate the failure of adjacent segments (Buttinelli et al., 2018; Walters et al., 2018, and references therein), fluid diffusion and overpressure are still retained the main mechanism to explain seismicity migration (Di Luccio et al., 2010; Malagnini et al., 2012; Miller et al., 2004; Sibson, 2000) and triggering of large aftershocks (Chiarabba & De Gori, 2009).

Our new models add to this discussion the reconnaissance of broad volumes with overpressurized fluids located at the base of the fault system (Figure 8). We observe peculiar low Vp and high Vp/Vs anomalies lying below the segments progressively activated since 1997, which become deeper and stronger southward. The two M_w6.1 and M_w6.5 mainshocks that occurred on 2016 are located on top of a broad high Vp/Vs volume present in the midcrust on the roof of which layered seismicity occurs. In the deep part of the faults, this anomaly is present before the starting of the sequence (Model B, Figure 8), suggesting that high pore pressure existed close to the incipient 2016 Amatrice and Norcia mainshocks. The higher Vp/Vs observed

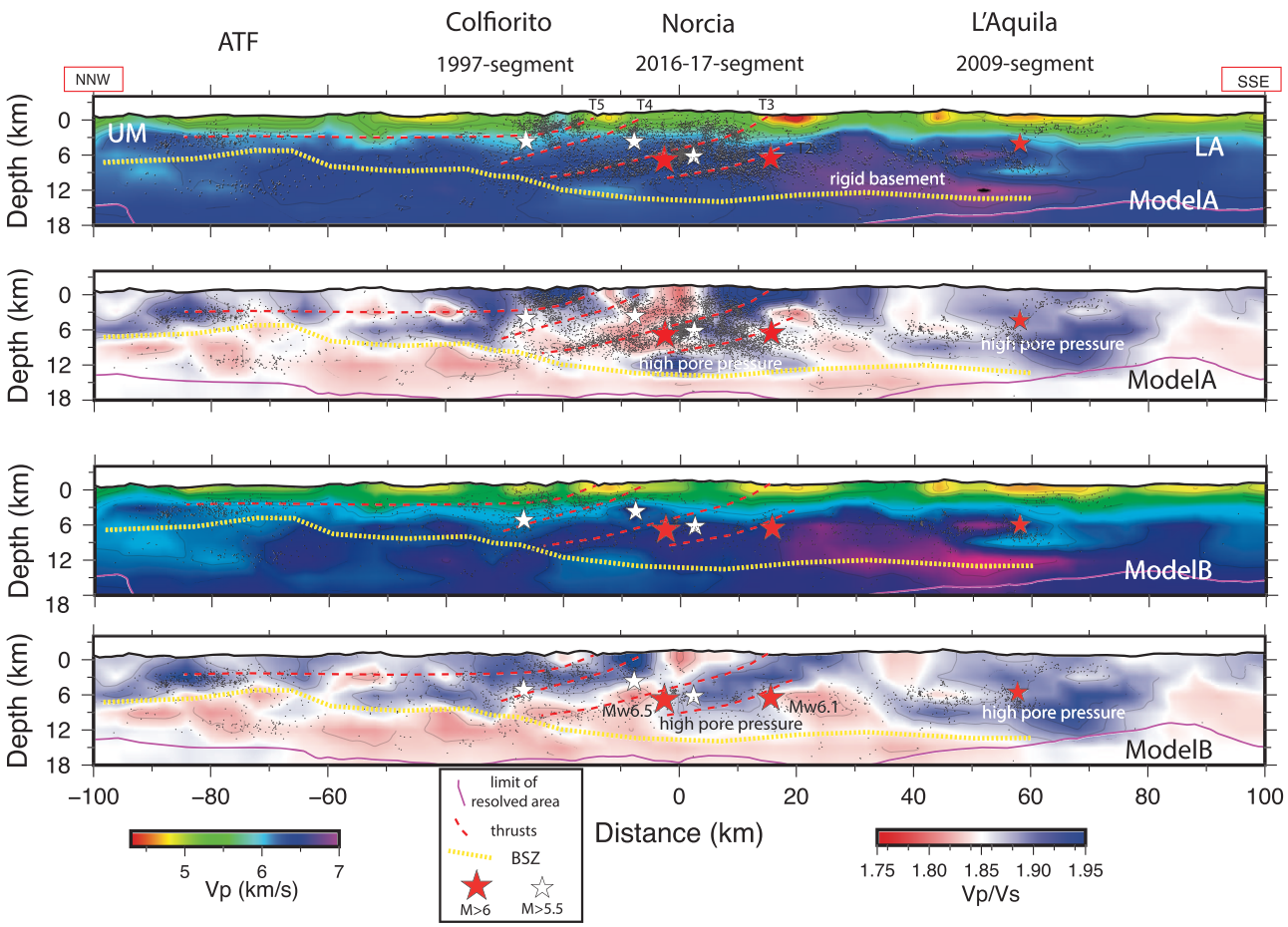

Figure 8. Vertical sections of Vp and Vp/Vs (for both Model A and Model B) and relocated seismicity (occurring ±10 km from section) along the normal faulting system. Stars are the $M > 5.6$ mainshocks; the red stars are the M_w6.1 and M_w6.5 2016 mainshocks. Purple lines are the limit of the resolved region (SF = 3.0). The yellow dashed line is the base of the normal faulting seismogenic layer. Seismicity is apparently present below this cutoff in the northern sector, since the projection of seismicity occurring on the east dipping decollement (see Figure 6, sections 1 and 2). Note the high Vp/Vs anomalies at the bottom of the layer and the pronounced anomalies in the hypocentral region of the 2016 mainshocks present before (Model B) and after the events (Model A).

in Model A vs Model B in this area, not associated to a change in Vp (Figure 8), although partially ascribable to a different volumetric sampling of the two models, could suggest a pore pressure increase during the 2016 coseismic period. We are attracted by this explanation that seems to be further supported by the intense seismicity observed on top of the anomaly, indicative of increasing cracking during the sequence, compatible with sustained fluid overpressure.

The overpressures around the base of the seismogenic zone may be related to the enormous CO_2 fluid flux being discharged (e.g., Chiodini et al., 2004), which can develop even in presence of high structural permeability. We hypothesize that fluids deeply permeate the midcrust, and their local upraise is partially hampered by the different permeability at the base of the seismogenic layer (Figure 8). This deep fluid leakage is a process active at the scale of the entire belt, from intense fluid surfacing in the stretched Tyrrhenian side to deep storing in the contractional Adriatic side, according to the different attitude of containment of fluid overpressure in different stress regimes (Sibson, 2003). In the still young and immature extensional belt, the intermittent overpressuring, with seismicity swarming within the east dipping layer, as seen either during the interseismic period (Carannante et al., 2013) and, with abrupt recrudescence, during the 2016 sequence. The final upraise of fluids within the shallow sedimentary cover (topmost 5 km) is compartmented within the inherited compressional structures, that create local overpressure in the footwall of the border normal faults. We hypothesize that the high Vp/Vs anomaly at the base of the seismogenic zone represents a

mixed H_2O-CO_2 fluid. We might argue that the greater compressibility of this mixed fluid, with respect to water, lies behind the partial recovery of the effect of fluid pressure on frictional behavior at the base of the seismogenic zone (e.g., Hirth & Beeler, 2015).

The process that we describe for the Apennines system could be exportable to other tectonic environments and cases of fluid-driven seismicity, both at local (e.g., induced seismicity) and regional scales (e.g., Sibson, 2014). Our study shows that fluid-filled volumes at the base of the seismogenic zone are persistent features within the crust and can be recognized with geophysical modeling. Transient increase of fluid pressure before earthquakes, not resolved in this study but suggested by the difference in Vp/Vs before and after the 2016 mainshocks, may be the target of detailed investigations. If fluid overpressure is prognostic of incipient ruptures on normal faults of the fault system, we can hope that significant signals could be caught in advance by dense systems of observations.

6. Conclusions

Lessons learned by recent earthquake sequences along the Apennines normal faulting system allow us to investigate interactions between fluids, crust heterogeneity, and seismicity. First, overpressured fluids pervaded the base of the seismogenic layer. All major sequences with mainshocks of $M > 5.5$ are related to broad volumes with high Vp/Vs pressurized fluids. In concomitance with the onset of the 2016 main ruptures, we find the first evidence of fluids upraise from the deep crust that enhanced cracking above a high Vp/Vs anomaly. Second, the extensional faults interested by seismicity represent the legacy of the segmentation of preexisting structures. The structural complexity derives from interaction between propagating thrusts and a rigid midcrustal body, generating a diffuse fault segmentation and the asymmetry of the belt observable at surface. The impediment of the rigid basement induced a regional rotation of thrusts, steep ramps and overcoming of structural highs in foreland positions while hampering the development of deeper thrust decollements.

This puzzle of reworked structures paves the floor to fluid assisted processes. Compartments with overpressurized fluids are limited and confined within the thrust sheets in the upper crust, perhaps floored and roofed by low permeability units which might locally enhance the overpressuring.

Large high Vp/Vs volumes at the base of the seismogenic layer are the main target for monitoring the interaction between deep fluids and seismicity before and during major seismic sequences, as well as in projects of underground exploitation. This could also help in developing physics-based forecast scenarios of seismic sequences.

Acknowledgments
Seismic data and waveforms can be retrieved from the EIDA database (https://www.orfeus-eu.org/data/eida/) by using the web services and tools available on the EIDA website. Authors declare no competing interests. We really thank Fabio Trippetta, Richard Sibson, an anonymous referee, and the Editors for the very constructive comments.

References

Baccheschi, P., De Gori, P., Villani, F., Trippetta, F., & Chiarabba, C. (2019). The preparatory phase of the M_w 6.1 2009 L'Aquila (Italy) normal faulting earthquake traced by foreshock time-lapse tomography. *Geology*, *48*(1), 49–55. https://doi.org/10.1130/G46618.1

Bally, A. W., Burbi, L., Cooper, C., & Ghelardoni, R. (1986). Balanced sections and seismic reflection profiles across the central Apennines. *Geological Evolution of the Mediterranean Basin*, *35*, 257–310.

Barchi, M. R., Alvarez, W., & Shimabukuro, D. H. (2012). The Umbria-Marche Apennines as a double orogen: Observations and hypotheses. *Italian Journal of Geosciences*, *131*(2), 258–271.

Bigi, S., Casero, P., & Ciotoli, G. (2011). Seismic interpretation of the Laga basin; constraints on the structural setting and kinematics of the central Apennines. *Journal of the Geological Society*, *168*(1), 179–190. https://doi.org/10.1144/0016-76492010-084

Bigi, S., & Costa Pisani, P. (2005). From a deformed Peri-Tethyan carbonate platform to a fold-and-thrust-belt: An example from the central Apennines (Italy). *Journal of Structural Geology*, *27*, 523–539.

Butler, R. W. H., Mazzoli, S., Corrado, S., De Donatis, M., Di Bucci, D., Gambini, R., et al. (2004). Applying thick-skinned tectonic models to the Apennine thrust belt of Italy: Limitations and implications. In K. R. McClay (Ed.), *Thrust tectonics and hydrocarbon systems, AAPG Memoirs*, (Vol. 82, pp. 647–667). Tulsa: Boulder.

Buttinelli, M., Pezzo, G., Valoroso, L., De Gori, P., & Chiarabba, C. (2018). Tectonics inversions, fault segmentation, and triggering mechanisms in the central Apennines normal fault system: Insights from high-resolution velocity models. *Tectonics*, *37*(11), 4135–4149. https://doi.org/10.1029/2018TC005053

Calamita, F., Paltrinieri, W., Pelorosso, M., Scisciani, V., & Tavarnelli, E. (2003). Inherited mesozoic architecture of the Adria continental paleomargin in the neogene central Apennines orogenic system, Italy. *Bollettino della Societa Geologica Italiana*, *122*, 307–318.

Carannante, S., Monachesi, G., Cattaneo, M., Amato, A., & Chiarabba, C. (2013). Deep structure and tectonics of the northern-central Apennines as seen by regional-scale tomography and 3-D located earthquakes. *Journal of Geophysical Research: Solid Earth*, *118*, 5391–5403. https://doi.org/10.1002/jgrb.50371

Chiarabba, C., & Amato, A. (2003). Vp and Vp/Vs images of the Colfiorito fault region (central Italy): A contribution to understanding seismotectonic and seismogenic processes. *Journal of Geophysical Research*, *108*(B5), 2248. https://doi.org/10.1029/2001JB001665

Chiarabba, C., Bagh, S., Bianchi, I., De Gori, P., & Barchi, M. (2010). Deep structural heterogeneities and the tectonic evolution of the Abruzzi region (central Apennines, Italy) revealed by microseismicity, seismic tomography, and teleseismic receiver functions. *Earth and Planetary Science Letters*, *295*(3-4), 462–476. https://doi.org/10.1016/j.epsl.2010.04.028

Chiarabba, C., & Chiodini, G. (2013). Continental delamination and mantle dynamics drive topography, extension and fluid discharge in the Apennines. *Geology*, *41*(6), 715–718.

Chiarabba, C., De Gori, P., Cattaneo, M., Spallarossa, D., & Segou, M. (2018). Faults geometry and the role of fluids in the 2016–2017 central Italy seismic sequence. *Geophysical Research Letters*, *45*, 6963–6971. https://doi.org/10.1029/2018GL077485

Chiarabba, C. P., & De Gori, E. B. (2009). Pore-pressure migration along a normal-fault system resolved by time-repeated seismic tomography. *Geology*, *37*, 67–70. https://doi.org/10.1130/G25220A.1

Chiaraluce, L., di Stefano, R., Tinti, E., Scognamiglio, L., Michele, M., Casarotti, E., et al. (2017). The 2016 central Italy seismic sequence: A first look at the mainshocks, aftershocks and source models. *Seismological Research Letters*, *88*(3), 757–771. https://doi.org/10.1785/0220160221

Chiodini, G., Cardellini, C., Amato, A., Boschi, E., Caliro, S., Frondini, F., & Ventura, G. (2004). Carbon dioxide Earth degassing and seismogenesis in central and southern Italy. *Geophysical Research Letters*, *31*, L07615. https://doi.org/10.1029/2004GL019480

D'Agostino, N., England, P., Hustand, I., & Selvaggi, G. (2014). Gravitational potential energy and active deformation in the Apennines, Earth planet. *Science Letters*, *397*, 121–132. https://doi.org/10.1016/j.epsl.2014.04.0130012

de Paola, N., Hirose, T., Mitchell, T., di Toro, G., Viti, C., & Shimamoto, T. (2011). Fault lubrication and earthquake propagation in thermally unstable rocks. *Geology*, *39*(1), 35–38. https://doi.org/10.1130/G31398.1

Di Luccio, F., Ventura, G., Di Giovambattista, R., Piscini, A., & Cinti, F. R. (2010). Normal faults and thrusts reactivated by deep fluids: The 6 April 2009 M_w 6.3 L'Aquila earthquake, central Italy. *Journal of Geophysical Research*, *115*, B06315. https://doi.org/10.1029/2009JB007190

Di Stefano, R., Chiarabba, C., Chiaraluce, L., Cocco, M., De Gori, P., Piccinini, D., & Valoroso, L. (2011). Fault zone properties affecting the rupture evolution of the 2009 (M_w 6.1) L'Aquila earthquake (central Italy): Insights from seismic tomography. *Geophysical Research Letters*, *38*, L10310. https://doi.org/10.1029/2011GL047365

di Toro, G., Han, R., Hirose, T., de Paola, N., Nielsen, S., Mizoguchi, K., et al. (2011). Fault lubrication during earthquakes. *Nature*, *471*(7339), 494–498. https://doi.org/10.1038/nature09

Dvorkin, J., Mavko, G., & Nur, A. (1999). Overpressure detection from compressional-and shear-wave data. *Geophysical Research Letters*, *26*, 3417–3420. https://doi.org/10.1029/1999GL008382

Guglielmi, Y., Cappa, F., Avouac, J. P., Henry, P., & Elsworth, D. (2015). *Science*, *348*(6240), 1224–1226. https://doi.org/10.1126/science.aab0476

Hainzl, S., & Ogata, Y. (2005). Detecting fluid signals in seismicity data through statistical earthquake modeling. *Journal of Geophysical Research*, *110*, B05S07. https://doi.org/10.1029/2004JB003247

Hainzl, S., Zöller, G., & Main, I. (2006). *Dynamics of seismicity patterns and earthquake triggering*. Elsevier.

Haslinger, F. (1998). Velocity structure, seismicity and seismotectonics of northwestern Greece between the Gulf of Arta and Zakynthos, PhD thesis, Dep. Geophys., ETH, Zurich, Switzerland.

Healy, J. H., Rubey, W. W., Griggs, D. T., & Raleigh, C. B. (1968). The Denver earthquakes. *Science*, *161*(3848), 1301–1310.

Hirth, G., & Beeler, N. M. (2015). The role of fluid pressure on frictional behavior at the base of the seismogenic zone. *Geology*, *43*, 223–226.

Improta, L., Bagh, S., de Gori, P., Valoroso, L., Pastori, M., Piccinini, D., et al. (2017). Reservoir structure and wastewater-induced seismicity at the Val d'Agri oilfield (Italy) shown by three-dimensional Vp and Vp/Vs local earthquake tomography. *Journal of Geophysical Research: Solid Earth*, *122*, 9050–9082. https://doi.org/10.1002/2017JB014725

Improta, L., De Gori, P., & Chiarabba, C. (2014). New insights into crustal structure, Cenozoic magmatism, CO_2 degassing, and seismogenesis in the southern Apennines and Irpinia region from local earthquake tomography. *Journal of Geophysical Research: Solid Earth*, *119*, 8283–8311. https://doi.org/10.1002/2013JB010890

Keranen, K. M., Weingarten, M., Abers, G. A., Bekins, B. A., & Ge, S. (2014). Sharp increase in central Oklahoma seismicity since 2008 induced by massive wastewater injection. *Science*, *345*(6195), 448–451. https://doi.org/10.1126/science.1255802

Lavecchia, G., Brozzetti, F., Barchi, M., Menichetti, M., & Keller, J. V. (1994). Seismotectonic zoning in east-central Italy deduced from an analysis of the Neogene to present deformations and related stress fields. *GSA Bulletin*, *106*(9), 1107–1120.

Llenos, A. L., & Michael, A. J. (2016). Characterizing potentially induced earthquake rate changes in the Brawley seismic zone, Southern California: Characterizing potentially induced earthquake rate changes in the Brawley seismic zone. *Bulletin of the Seismological Society of America*, *106*(5), 2045–2062. https://doi.org/10.1785/0120150053

Lombardi, A. M., Cocco, M., & Marzocchi, W. (2010). On the increase of background seismicity rate during the 1997–1998 Umbria-Marche, central Italy, sequence: Apparent variation or fluid-driven triggering? *Bulletin of the Seismological Society of America*, *100*, 1138–1152. https://doi.org/10.1785/0120090077

Lucente, F. P., De Gori, P., Margheriti, L., Piccinini, D., Di Bona, M., Chiarabba, C., & Piana, A. N. (2010). Temporal variation of seismic velocity and anisotropy before the 2009 M_W 6.3 L'Aquila earthquake, Italy. *Geology*, *38*, 1055–1056. https://doi.org/10.1130/focus112010.1

Malagnini, L., Lucente, F. P., De Gori, P., Akinci, A., & Munafò, I. (2012). Control of pore fluid pressure diffusion on fault failure mode: Insights from the 2009 L'Aquila seismic sequence. *Journal of Geophysical Research*, *117*, B05302. https://doi.org/10.1029/2011JB008911

Mancinelli, P., Porreca, M., Pauselli, C., Minelli, G., Barchi, M. R., & Speranza, F. (2019). Gravity and magnetic modeling of central Italy: Insights into the depth extent of the seismogenic layer. *Geochemistry, Geophysics, Geosystems*, *20*, 2157–2172. https://doi.org/10.1029/2018GC008002

Mazzoli, S., Deiana, F., Galdenzi, S., & Cello, G. (2002). Miocene fault-controlled sedimentation and thrust propagation in the previously faulted external zones of the Umbria–Marche Apennines, Italy. *EGU Stephan Mueller Special Publication Series*, *1*, 195–209.

Miller, S. A., Collettini, C., Chiaraluce, L., Cocco, M., Barchi, M., & Kaus, B. J. (2004). Aftershocks driven by a high-pressure CO_2 source at depth. *Nature*, *427*(6976), 724–727. https://doi.org/10.1038/nature02251

Mirabella, F., Brozzetti, F., Lupattelli, A., & Barchi, M. R. (2011). Tectonic evolution of a low angle extensional fault system from restored cross sections in the northern Apennines (Italy). *Tectonics*, *30*, TC6002. https://doi.org/10.1029/2011TC002890

Nur, A., & Booker, J. R. (1972). Aftershocks caused by pore fluid flow? *Science*, *175*, 885–887.

Parotidis, M., Rothert, E., & Shapiro, S. A. (2003). Pore-pressure diffusion: A possible triggering mechanism for the earthquake swarms 2000 in Vogtland/NW-Bohemia, central Europe. *Geophysical Research Letters*, *30*(20), 2075. https://doi.org/10.1029/2003GL018110

Peterie, S. L., Miller, R. D., Intfen, J. W., & Gonzales, J. B. (2018). Earthquakes in Kansas induced by extremely far-field pressure diffusion. *Geophysical Research Letters*, *45*, 1395–1401. https://doi.org/10.1002/2017GL076334

Raleigh, C. B., Healy, J. H., & Bredehoeft, J. D. (1976). An experiment in earthquake control at Rangely, Colorado. *Science*, *191*(4233), 1230–1237. https://doi.org/10.1126/science.191.4233.1230

Reches, Z., & Lockner, D. A. (2010). Fault weakening and earthquake instability by powder lubrication. *Nature*, *467*(7314), 452–455. https://doi.org/10.1038/nature09348

Savage, M. K. (2010). The role of fluids in earthquake generation in the 2009 M_w 6.3 L'Aquila, Italy, earthquake and its foreshocks. *Geological Society of America*, *38*(11), 1055–1056. https://doi.org/10.1130/focus112010.1

Scisciani, V., Agostini, S., Calamita, F., Pace, P., Cilli, A., Giori, I., & Paltrinieri, W. (2014). Positive inversion tectonics in foreland fold-and-thrust belts: A reappraisal of the Umbria–Marche northern Apennines (central Italy) by integrating geological and geophysical data. *Tectonophysics*, *637*, 218–237.

Shapiro, S. (2015). *Fluid-induced seismicity*. Cambridge: Cambridge University Press. https://doi.org/10.1017/CBO9781139051132

Shapiro, S. A., Patzig, R., Rothert, E., & Rindschwentner, J. (2003). Triggering of seismicity by pore pressure perturbations: Permeability related signatures of the phenomenon. *Pure and Applied Geophysics*, *160*, 1051–1066.

Sibson, R. (2000). Fluid involvement in normal faulting. *Journal of Geodynamics*, *29*, 469–499. https://doi.org/10.1016/S0264-3707(99)00042-3

Sibson, R. (2003). Brittle-failure controls on maximum sustainable overpressure in different tectonic regimes. *AAPG Bulletin*. *87*. 901–908. https://doi.org/10.1306/01290300181.

Sibson, R. (2014). Earthquake rupturing in fluid-overpressured crust: How common? *Pure and Applied Geophysics*, *171*. https://doi.org/10.1007/s00024-014-0838-3

Sleep, N., & Blanpied, M. (1992). Creep, compaction and the weak rheology of major faults. *Nature*, *359*, 687–692.

Stein, R. S. (1999). The role of stress transfer in earthquake triggering. *Nature*, *402*, 605–609.

Takei, Y. (2002). Effect of pore geometry on Vp/Vs: From equilibrium geometry to crack. *Journal of Geophysical Research: Solid Earth*, *107*(B2), ECV-6.

Tavarnelli, E., Butler, R. W. H., Decandia, E. A., Calamita, F., Grasso, M., Alvarez, W., & Renda, P. (2004). Implications of fault reactivation and structural inheritance in the Cenozoic tectonic evolution of Italy. In U. Crescenti, S. D'Offizi, S. Merlini, & R. Sacchi (Eds.), *The nature and tectonic significance of fault zone weakening, Special Publications*, (Vol. 186, pp. 273–286). London: Geological Society.

Trippetta, F., Carpenter, B. M., Mollo, S., Scuderi, M. M., Scarlato, P., & Collettini, C. (2017). Physical and transport property variations within carbonate-bearing fault zones: Insights from the Monte Maggio fault (central Italy). *Geochemistry, Geophysics, Geosystems*, *18*, 4027–4042. https://doi.org/10.1002/2017GC007097

Trippetta, F., Collettini, C., Vinciguerra, S., & Meredith, P. G. (2010). Laboratory measurements of the physical properties of Triassic evaporites from central Italy and correlation with geophysical data. *Tectonophysics*, *492*(1–4), 141–149.

Valoroso, L., Chiaraluce, L., Di Stefano, R., & Monachesi, G. (2017). Mixed-mode slip behavior of the Altotiberina low-angle normal fault system (northern Apennines, Italy) through high-resolution earthquake locations and repeating events. *Journal of Geophysical Research: Solid Earth*, *122*, 10,220–10,240. https://doi.org/10.1002/2017JB014607

Vezzani, L. & Festa, A. & Ghisetti, F. (2010). Geology and tectonic evolution of the central-southern Apennines, Italy.

Walters, R. J., Gregory, L. C., Wedmore, L. N. J., Craig, T. J., McCaffrey, K., Wilkinson, M., et al. (2018). Dual control of fault intersections on stop-start rupture in the 2016 central Italy seismic sequence. *Earth and Planetary Science Letters*, *500*, 1–14, ISSN 0012-821X. https://doi.org/10.1016/j.epsl.2018.07.043

Yeck, W. L., Weingarten, M., Benz, H. M., McNamara, D. E., Bergman, E. A., Herrmann, R. B., et al. (2016). Far-field pressurization likely caused one of the largest injection induced earthquakes by reactivating a large preexisting basement fault structure. *Geophysical Research Letters*, *43*, 10,198–10,207. https://doi.org/10.1002/2016GL070861

Yu, H., Harrington, R. M., Liu, Y., & Wang, B. (2019). Induced seismicity driven by fluid diffusion revealed by a near-field hydraulic stimulation monitoring array in the Montney Basin, British Columbia. *Journal of Geophysical Research: Solid Earth*, *124*, 4694–4709. https://doi.org/10.1029/2018JB017039

Zhao, D., Kanamori, H., & Negishi, H. (1996). Tomography of the source area of the 1995 Kobe earthquake: Evidence for fluids at the hypocenter? *Science*, *274*, 1891–1894.

Zhao, D., Kitagawa, H., & Toyokuni, G. (2015). A water wall in the Tohoku forearc causing large crustal earthquakes. *Geophysical Journal International*, *200*(1), 149–172. https://doi.org/10.1093/gji/ggu381

Zoback, M., & Harjes, H. (1997). Injection-induced earthquakes and crustal stress at 9 km depth at the KTB deep drilling site, Germany. *Journal of Geophysical Research*, *102*(B8), 18,477–18,491.